Published in Ground Water 47, issue 3, 361-369, 2008
which should be used for any reference to this work

Percolation and Particle Transport in the Unsaturated Zone of a Karst Aquifer

Michiel Pronk[1], Nico Goldscheider[2], Jakob Zopfi[3], and François Zwahlen[1]

Abstract

Recharge and contamination of karst aquifers often occur via the unsaturated zone, but the functioning of this zone has not yet been fully understood. Therefore, irrigation and tracer experiments, along with monitoring of rainfall events, were used to examine water percolation and the transport of solutes, particles, and fecal bacteria between the land surface and a water outlet into a shallow cave. Monitored parameters included discharge, electrical conductivity, temperature, organic carbon, turbidity, particle-size distribution (PSD), fecal indicator bacteria, chloride, bromide, and uranine. Percolation following rainfall or irrigation can be subdivided into a lag phase (no response at the outlet), a piston-flow phase (release of epikarst storage water by pressure transfer), and a mixed-flow phase (increasing contribution of freshly infiltrated water), starting between 20 min and a few hours after the start of recharge event. Concerning particle and bacteria transport, results demonstrate that (1) a first turbidity signal occurs during increasing discharge due to remobilization of particles from fractures (pulse-through turbidity); (2) a second turbidity signal is caused by direct particle transfer from the soil (flow-through turbidity), often accompanied by high levels of fecal indicator bacteria, up to 17,000 *Escherichia coli*/100 mL; and (3) PSD allows differentiation between the two types of turbidity. A relative increase of fine particles (0.9 to 1.5 μm) coincides with microbial contamination. These findings help quantify water storage and percolation in the epikarst and better understand contaminant transport and attenuation. The use of PSD as "early-warning parameter" for microbial contamination in karst water is confirmed.

Introduction

The unsaturated zone of karst aquifers, consisting of the soil, epikarst, and a transmission zone, plays a crucial role for ground water recharge and contaminant attenuation. Significant amounts of (plant accessible) water and contaminants can be stored in this zone for prolonged periods of time, allowing for biodegradation and other attenuation processes to operate. However, due to flow concentration in the epikarst, water and contaminants can also be rapidly transported downward to the active conduit network, often via vertical shafts, mainly during storm rainfall (Klimchouk 2004; Williams 2008).

Not only water and solutes but also different types of organic and inorganic particles and colloids can be transported through karst systems. Sediments in karst systems can act as reservoirs for contaminants, such as dense non-aqueous phase liquids, pesticides, and toxic metals. During storm events, they can be mobilized and transported toward springs or wells (Loop and White 2001; Vesper and White 2003, 2004). Particles also act as transport vectors for microbial pathogens, generally originating from human activities at the land surface, such as agriculture or waste water releases (Mahler et al. 2000; Ryan and Meiman 1996).

Suspended particles and colloids are often measured as turbidity. Turbidity at karst springs may result either from the remobilization of intrakarstic sediments due to

[1] Center of Hydrogeology, University of Neuchâtel, Rue Emile-Argand 11, CH-2009 Neuchâtel, Switzerland.
[2] Corresponding author: Center of Hydrogeology, University of Neuchâtel, Rue Emile-Argand 11, CH-2009 Neuchâtel, Switzerland; (41) 32 718 2645; fax: (41) 32 718 2604; nico.goldscheider@unine.ch
[3] Laboratory of Microbiology, Institute of Biology, University of Neuchâtel, Rue Emile-Argand 11, CH-2009 Neuchâtel, Switzerland.

increased flow velocities (pulse-through or autochthonous turbidity) or from direct transfer from the land surface (flow-through or allochthonous turbidity) (e.g., Mahler and Lynch 1999; Massei et al. 2003). The first type of turbidity often occurs shortly after the rain, during increasing flow, while the second turbidity signal may arrive hours to several days later, depending on the flow-through time, often during the recession phase (Pronk et al. 2006). Turbidity is a bulk optical parameter, while particle-size distribution (PSD) measurements (Atteia and Kozel 1997; Mahler and Lynch 1999) and mineralogical analyses (Herman et al. 2007) yield more detailed information about the number, size, and composition of particles in karst spring water.

Recently, it was demonstrated that continuous monitoring of PSD in karst spring water can also be used to differentiate between both types of turbidity: pulse-through turbidity is characterized by an increase of all particle-size classes, whereas flow-through turbidity can be identified by a relative increase of small particles (~1 μm), which are not or only slightly affected by sedimentation. Fecal bacteria contamination is often associated with this type of turbidity, because they also originate from the land surface, so that PSD was proposed as an "early-warning parameter" for microbial contamination of karst spring water (Pronk et al. 2007). Artificial tracer tests with solutes and colloids/particles also confirmed that particles of a similar size as bacteria (~1 μm) and *Cryptosporidium* cysts (3 to 7 μm) can travel over large distances in karst systems, even during low-flow conditions (Göppert and Goldscheider 2008).

In general, the role of sediments in contaminant storage, attenuation, and transport in karst aquifers has not been sufficiently investigated and would require more research (White 2002). The few available studies cited earlier mainly deal with sediment transport in the main conduit network, whereas investigations of the epikarst mostly focused on the percolation of water and solute transport (Perrin et al. 2003; Savoy 2007). Colloid transport, on the other hand, was mostly studied in porous media, whereas there is little knowledge about the behavior of particles, colloids, and associated contaminants in the unsaturated zone of karst aquifers (McCarthy and McKay 2004).

Therefore, the objectives of the present study were (1) to characterize and differentiate the two principal components, storage water and freshly infiltrated water, contributing to percolation in the unsaturated zone of a karst aquifer; (2) to investigate the temporal variations of sediment particles in this zone in response to recharge events, with the main focus on the mobilization and transfer of particles and the associated microbial contaminants; (3) to identify the processes governing particle dynamics and transport; and (4) to further confirm (or refute) the use of PSD as an early-warning parameter for fecal contamination, as it can be done for karst spring water.

To achieve these goals, several irrigation and tracing experiments were carried out between 2005 and 2007 at three sites in the Swiss Jura Mountains: the artificial galleries near Gänsbrunnen (Canton Solothurn) and the Grand-Bochat and the Vers-chez-le-Brandt caves (Canton Neuchâtel). The latter was also continuously monitored to observe the response of natural parameters at the cave outlet to rainfall events. Ready access and the simple setting make this cave a suitable site for this type of investigation. The most complete and insightful results were obtained at the Vers-chez-le-Brandt cave; therefore, mainly the findings from this test site will be presented here.

Methodology

Test Site, Instrumentation, and Experimental Setup

The nearly horizontal Vers-chez-le-Brandt cave is developed in Upper Jurassic limestone beneath relatively flat pastureland. About 1 to 2 m of soil/loess and 30 m of limestone overlie the 200-m-long cave (Figure 1). In terms of soil, land use, and lithology, this setting is quite typical for large parts of the Jura Mountains. A perennial vadose flow issuing from a fracture at the cave roof was monitored and sampled. The base flow of this outlet is approximately 0.6 L/min. The study consisted of three elements:

- Continuous monitoring of natural parameters at the outlet for several months
- A long-term (steady-state) irrigation and tracer experiment
- A short-term (transient) irrigation experiment (without artificial tracers).

To study the response of the unsaturated zone to natural rainfall events, discharge, temperature, electrical conductivity (EC), turbidity, and total organic carbon (TOC) were monitored continuously from June to November 2007. Discharge was measured by collecting water from the fracture on a plastic sheet draining toward a flow gauge containing a pressure probe (RTC28; Kistler, Winterthur, Switzerland); temperature and EC were monitored using a conductivity probe (340i; WTW, Weilheim, Germany) and recorded every 2 min by data loggers (DT50; dataTaker, Rowville, Australia). Turbidity and TOC were measured every 30 s with a GGUN-FL30 fluorometer (Schnegg and Costa 2003).

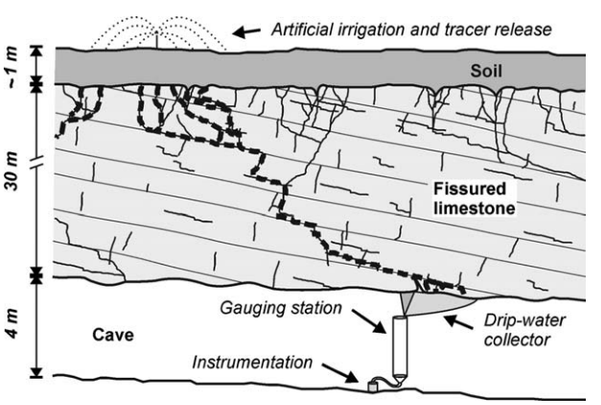

Figure 1. Schematic section of the test site and illustration of the experimental setup.

The irrigation (and tracer) experiments were done using garden sprinklers connected to a pump and a reservoir of 6 m^3. The irrigated areas were chosen according to previous studies, which established the catchment of the monitored outlet by means of tracer tests (Perrin 2003; Savoy 2007). In addition to the standard monitoring program presented earlier, PSD was determined every 2 min with a portable particle counter (Abakus mobil fluid; Klotz, Unterhaugstett, Germany) that groups the particles into 32 definable size classes ranging from 0.9 to 139 μm. Uranine was monitored continuously with the aforementioned fluorometer at a time step of 30 s, and samples were collected for major ion chemistry and fecal indicator bacteria (*Escherichia coli* and enterococci). Major ion chemistry was analyzed by ion chromatography (DX-120; Dionex, Sunnyvale, California); fecal indicator bacteria were determined, within 20 h after sampling, using standard cultivation techniques (APHA, AWWA, and WEF 2005).

The long-term irrigation and tracer experiment in September 2005 had a twofold goal: characterizing the flow conditions in the unsaturated zone and studying particle and solute transport. An area of 28 m^2 (which is only a part of the outlet catchment) was irrigated for 13.2 h at a constant rate of 7.1 L/min, corresponding to an intensity of 15.1 mm/h or 200 mm of rain. With respect to the typical scale of regional fracture frequencies and epikarst development, this irrigation area is supposed to be sufficiently large to obtain results that are representative for larger areas. When stable conditions were reached, two successive tracer tests were carried out. For both tests, 35 L of water containing the tracers was pumped through the irrigation device, and the irrigation was continued afterward. A quantity of 300 g of bromide (Br^-) in the form of NaBr was released 3.3 h after the start of the irrigation after 7.1 h, 518 mg of uranine and 3.6 L of clayey loam suspension were released (the suspension was obtained from sediments at a karst spring in the region). The PSD of this injected suspension was determined using the particle counter (Figure S1); the suspension included a total number of approximately 8×10^{11} particles.

The short-term irrigation experiment in October 2007 was designed to study the behavior of particles, TOC, and fecal bacteria with an irrigation scenario similar to natural rain events. A volume of 670 L of water was irrigated on an area of 28 m^2 during 1.5 h at a constant rate of 7.4 L/min, corresponding to an intensity of 15.8 mm/h and a total rainfall of 23.7 mm. No artificial tracers were released during this experiment.

Long dry periods preceded both experiments (11 and 8 d for the September 2005 and October 2007 experiments, respectively), resulting in an outlet discharge close to its base flow. For both experiments, tap water was used for irrigation; it had a pH of 7.3, an EC close to the water discharging from the outlet during dry periods (~500 μS/cm), and very low background levels of the parameters monitored at the outlet (turbidity: 0.2 to 0.4 nephelometric turbidity unit [NTU], TOC: 0.6 to 0.8 mg/L, and *E. coli* and enterococci: 0 to 1 colony-forming units [CFU]/100 mL).

Hydrograph Separation for the Irrigation Experiments

It is assumed that the outlet discharge Q_O is the result of mixing of two components: storage water Q_S that is released by gravity drainage and pressure transfer and freshly infiltrated water that directly percolates from the soil surface through the unsaturated zone and discharges at the outlet, noted as Q_D. Two equations describe the water fluxes and the corresponding natural tracer concentrations (c_O, c_S, and c_D):

$$Q_O = Q_S + Q_D \tag{1}$$

$$Q_O c_O = Q_S c_S + Q_D c_D \tag{2}$$

For conservative tracers, c_D is equal to the concentration in the infiltration water (c_I). Combining Equations (1) and (2) makes it possible to quantify, at any instant in time, the contribution of freshly infiltrated water to the discharge at the outlet via direct transfer:

$$Q_D = \frac{c_O - c_S}{c_D - c_S} Q_O \tag{3}$$

The corresponding water volumes (V_O, V_D, V_S, and V_I) were calculated by integrating the respective discharges over time. In this study, chloride was used as a conservative tracer, which is present both in the natural system and in the irrigation water. This approach assumes that the chloride concentration of the storage component (c_S) remains constant throughout the experiment. Preliminary irrigation experiments, using constant bromide (absent in storage water) and chloride concentrations in the irrigation water, demonstrated the validity of this hypothesis (Figure S2).

Results and Discussion

Natural Rainfall Events

The responses of the water outlet to a small rainfall event (2.8 mm during 1.5 h) and to a major rainfall event (19.1 mm in 8 h) are shown in Figure 2. Because both events were preceded by dry periods of 5 d, the initial discharge of the outlet was close to its base flow at 0.7 L/min. The hydrographs showed a rapid increase, starting about 2 h after the start of the rain, followed by slow recession. The maximum discharge was 2.0 L/min during the small rainfall and about 100 L/min during the intense rainfall event.

The arrival of freshly infiltrated rain water at the outlet, indicated by sudden decreases in EC, occurred about 160 and 20 min after the initial discharge increases for the small and intense rainfall events, respectively. These flow-through times corresponded well to the discharge-dependent transit time relationship obtained from artificial and natural tracer tests (Figure S3). Simultaneously to the arrival of fresh infiltration water, TOC, principally originating from the soil, started to increase. Flow

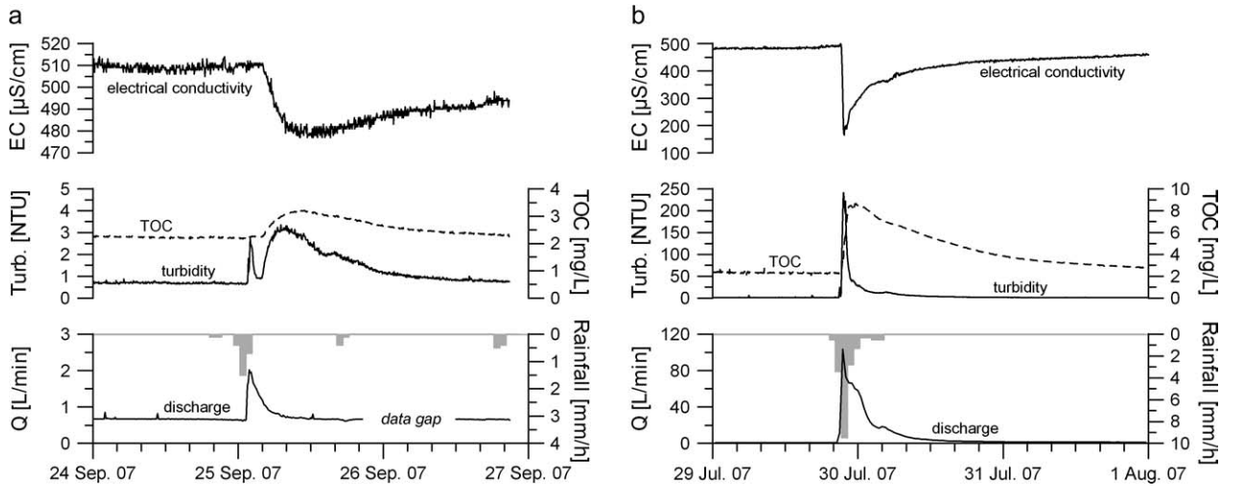

Figure 2. Responses to natural rainfall events monitored at the water outlet in the cave: (a) small rainfall event and (b) abundant rainfall event. *Q*, discharge; Turb., turbidity.

variations in the unsaturated zone may thus be divided into three phases: (I) a lag phase, where rainfall has already occurred, but the outlet shows no reaction. The duration of this phase depends largely on the initial saturation of the soil; (II) a piston phase, starting at the moment of discharge increase and lasting until the arrival of fresh infiltration water. Water discharging during this phase originates from the epikarst, released by a pressure pulse produced by increasing hydraulic head; and (III) a mixing phase, where water discharging at the outlet is a mixture of epikarst water, soil water, and rain water.

The volumes of the different components feeding the outlet are difficult to quantify. However, the volume of epikarst water discharging at the outlet represented at least 73% and 26% (calculated during phase II) of the total water volume discharged during the small and large precipitation events, respectively. This high contribution of storage water during rainfall events has also been observed in other studies (Lee and Krothe 2001; Perrin et al. 2003), where it represented about 70% to 90%.

The turbidity variations during the two events differed significantly. During the small rainfall event (Figure 2a), two distinct successive turbidity signals were observed: a first signal during the rising limb of the hydrograph while EC and TOC remained stable at preevent levels and a second much wider turbidity signal during flow recession, accompanied by a simultaneous EC decrease and TOC increase. The first signal is attributed to the mobilization and scouring of particles inside fractures, close to the outlet, by increasing flow velocities and turbulences resulting from pressure transfer, that is, pulse-through turbidity; the second signal indicates the arrival of freshly infiltrated rain water that mobilized soil particles by hydrodynamic shear, that is, flow-through turbidity.

During the major rainfall event (Figure 2b), turbidity seemed to display only one large signal increasing simultaneously with discharge. However, observing the turbidity graph in detail, two turbidity events can be distinguished as during the small rainfall event: a first signal, that is, pulse-through turbidity, reached a maximum of 24 NTU about 10 min after the start of discharge increase and recessed to 4 NTU. Simultaneous with the arrival of freshly infiltrated water, only about 20 min after the initial discharge increase, a flow-through turbidity signal increased and reached a maximum of 240 NTU about 15 min after peak discharge. Therefore, the very large and early flow-through turbidity signal largely masked the much smaller pulse-through turbidity signal. Substantial amounts of sediments may thus be released from the soil and epikarst during intense and abundant rainfall events and transported to the active conduit network of karst systems.

During both events, the turbidity transported by infiltration water (flow-through turbidity) preceded the corresponding TOC signals, although both turbidity and TOC originate from the soil. This observation is consistent with findings from other studies, which revealed faster transport of particles and colloids with respect to solutes due to exclusion mechanisms in porous media (Sirivithayapakorn and Keller 2003), fractures (Zvikelsky and Weisbrod 2006), and karst conduits (Göppert and Goldscheider 2008).

Characterization of Flow in the Unsaturated Zone

The outlet response to the long-term irrigation experiment (Figure 3) allowed for the characterizing and quantifying of flow within the unsaturated zone (the results of the tracer test done during this experiment will be discussed in the next section). Several phases, reflecting the changes in flow conditions and contributing components, were distinguished and enabled a “phase-by-phase” conceptual model to be proposed (Figure 4). The model considers three types of fissures/fractures differing in their hydrological function resulting mainly from the aperture width, and it is based on the different types of water flow occurring in the unsaturated zone (Klimchouk 2004; Kogovšek 1997): (1) small fissures, which have not been affected by dissolution processes; they are always saturated

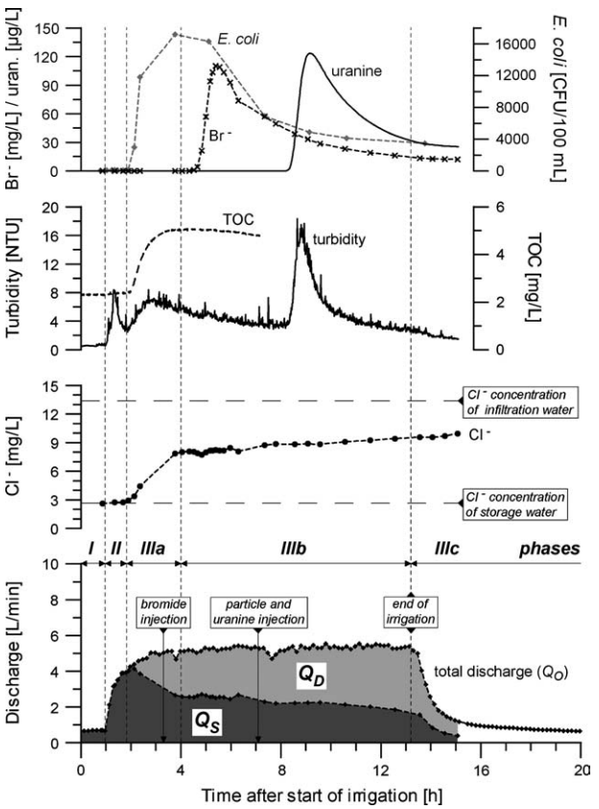

Figure 3. Results of the long-term irrigation experiment. The response of the water outlet in the cave can be divided into several phases distinguished by different flow conditions and contributions of storage water (Q_S) and direct transfer of infiltration water (Q_D), which were separated using chloride concentrations. The third turbidity peak (with a maximum about 18 NTU) corresponds to the breakthrough of the comparative tracer test (clayey loam suspension and uranine, for details see Figure 5).

with water that can move only by pressurized flow and are characterized by vadose seepage; (2) medium fissures, which are saturated during high recharge conditions and allow for moderately fast percolation or vadose flow; and (3) large fractures, which are never fully saturated and allow for rapid gravitational percolation or shaft flow. The outlet is connected to such a solutionally enlarged fracture.

Because the experiment was preceded by a long dry period, the discharge of the outlet (0.7 L/min) was stable and close to its base flow value. It is thus hypothesized that the soil water was immobile (i.e., soil water content less than field capacity). Therefore, the water percolating at the outlet results from the slow gravity drainage of epikarst water (*Qs*) from medium fractures via large fractures toward the outlet. When irrigation started, all parameters remained stable at preexperimental levels (Figure 3, phase I). During this lag phase, the irrigation water is essentially used to replenish the soil water deficit (Figure 4a).

The piston phase (Figure 3, phase II) started after 0.9 h of irrigation with a sudden discharge increase from 0.7 to 3.9 L/min, whereas chloride and TOC remained stable, indicating that the water discharging at the outlet is still composed entirely of storage water. This is attributed to a pressure pulse from the soil water column, causing water transfer from small and medium fissures into larger fissures (Figure 4b). Turbidity increased simultaneously to discharge, reached a maximum of 8.4 NTU before the discharge maximum, and then decreased to 2.5 NTU. This pulse-through turbidity results from the mobilization and scouring of particles in the large fractures near the outlet due to increasing flow velocities.

The mixing phase (phase III) is characterized by a mixed contribution of epikarst and soil storage water (Q_S) and direct transfer of freshly infiltrated water (Q_D). Phase III can further be subdivided into three stages.

Phase IIIa starts after 1.9 h of irrigation and is defined by the first arrival of infiltration water, demonstrated by an increase of chloride, and soil water, demonstrated by an increase of TOC. The still increasing discharge and the rapidly changing chloride concentration at the outlet demonstrate the transient character of this phase. Such a fast direct transfer of water (approximately 16 m/h) is possible only via large fractures (Figure 4c). The decreasing storage water (Q_S) discharging at the outlet is explained by a decreasing drainage of the medium and small fissures into the larger fractures, possibly resulting from a hydraulic gradient inversion. Simultaneous with the first arrival of fresh infiltration water, a second turbidity episode was monitored at the outlet. Turbidity reached a maximum of 7.1 NTU after 2.8 h of irrigation and then decreased until the end of the experiment. This is clearly flow-through turbidity, that is, direct transfer of eroded soil particles from the land surface and soil zone, also confirmed by a dramatic increase of *E. coli* levels up to 17,000 CFU/100 mL.

Transition between phases IIIa and IIIb is marked by a sudden decrease in the slope of the increasing chloride concentration, coinciding with a stabilization of the outlet discharge at about 5.2 L/min (Figure 3). This observation suggests the establishment of steady-state flow conditions with a high level of water saturation in the soil and well-organized flow routes through a network of small, medium, and large fractures (Figure 4d). The continuing gradual increase of chloride concentrations, suggesting a slightly decreasing drainage of storage water and an increasing contribution of infiltration water, expresses the effect of mixing between storage and infiltration water in the medium and smaller fissures.

Phase IIIc is the recession period after irrigation was stopped. The discharge decreased rapidly due to decreasing hydraulic heads. However, the still slightly increasing chloride concentration (Figure 3) suggests a higher degree of drainage of the large fractures, which mainly include irrigation water rich in chloride, with respect to drainage of the medium and small fissures containing a mixture of infiltration water and storage water, which includes less chloride (Figure 4e).

The discharge at the outlet (Q_O) during steady-state flow conditions (phase IIIb) represented about 73% of the irrigation rate (Q_I). Obviously, the missing 27% of water used another, unmonitored percolation pathway, presumably laterally bypassing the cave. During another

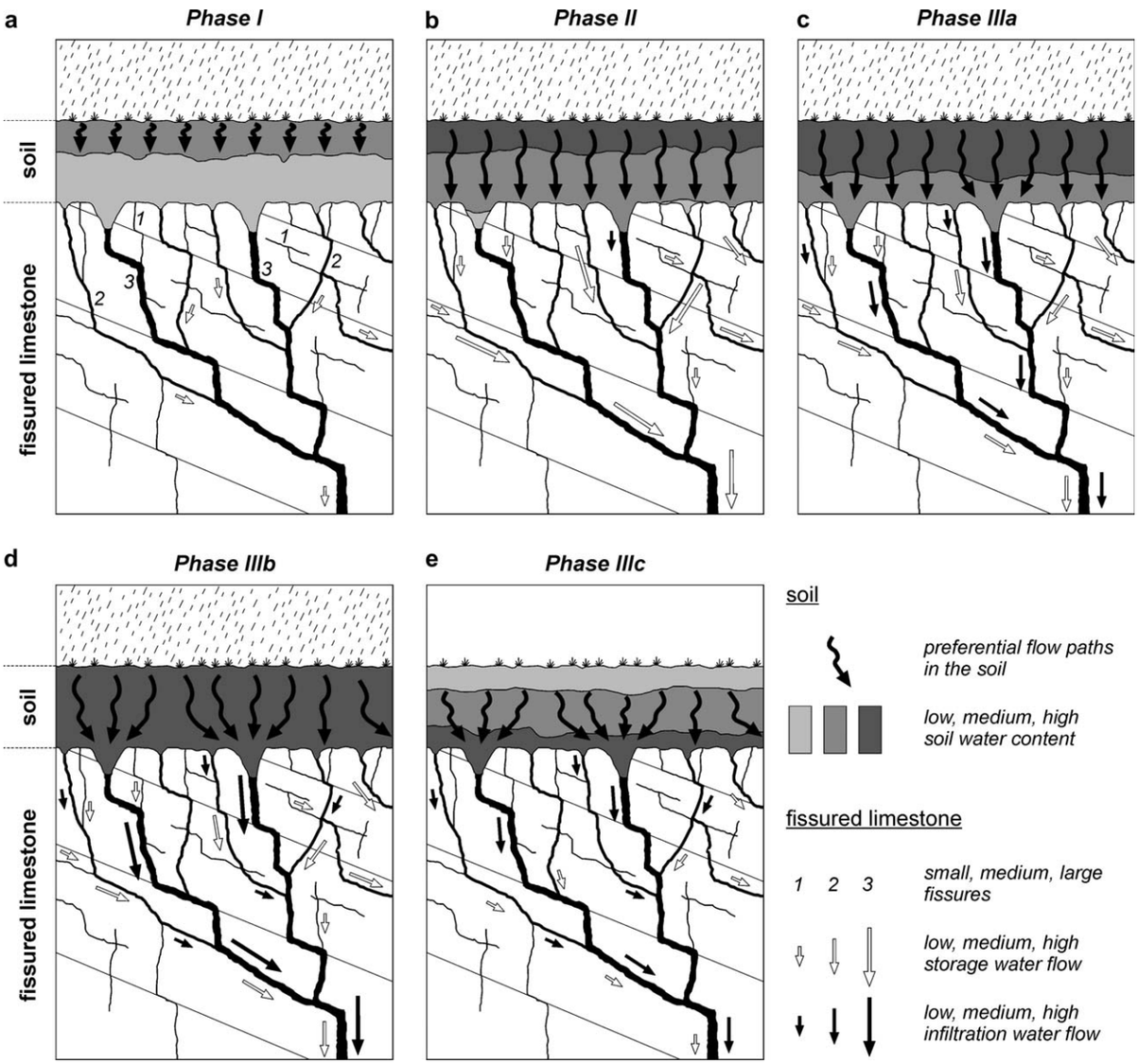

Figure 4. Conceptual model of flow routes and percolation conditions during the long-term irrigation experiment (or during very long and abundant rainfall events).

experiment at this site, with a smaller irrigation area, the outlet discharge was 99% of the infiltration rate, suggesting a more focused percolation with nearly no lateral losses.

During the entire experiment, 36% of the irrigated water volume (V_I) reached the cave via direct transfer (V_D obtained by integration of Q_D). This value is very close to the recovery of bromide, which was injected as a conservative artificial tracer during the experiment: 39% (Figure 3). The total volume of infiltration water that reached the outlet via direct transfer (V_D) was approximately 2.0 m^3 and the volume of storage water (V_S) was also approximately 2.0 m^3. Redistributed on 28 m^2 (surface of the irrigation area), this corresponds to 70 mm of water storage. Extrapolation of the linear chloride and discharge trends makes it possible to estimate the total volume of storage water: 3.1 m^3 or 110 mm.

Comparative Tracer Test during Steady-State Flow Regime

When steady-state flow conditions were reached in the system (Figure 3, phase IIIb), a mixture of uranine and clayey loam suspension was released at the surface 7.1 h after the experiment began and monitored at the outlet (Figure 5). Uranine was first detected at the outlet 1.1 h after tracer release and reached a maximum of 123 µg/L after 2.1 h. The uranine breakthrough curve (BTC) shows a long tail, and the tracer was still detectable at the end of the monitoring period. Monitored uranine recovery reached 22%. However, extrapolation of the BTC suggests that the total uranine recovery should approach the bromide recovery about 39%.

All particle-size classes between 0.9 and 8.0 µm showed a positive response to the release of the suspension. Particles larger than 3.5 µm showed irregular BTCs

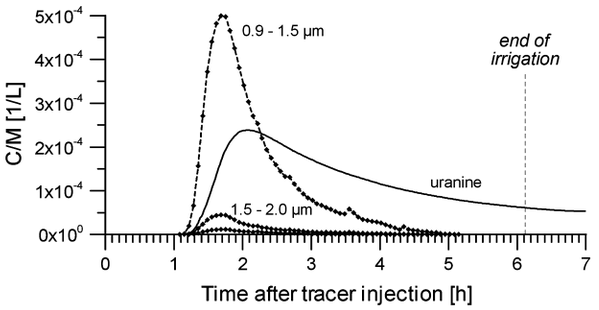

Figure 5. Results of the comparative tracer test during steady-state flow regime of the long-term irrigation experiment. Only the BTCs for uranine and the 0.9 to 1.5, 1.5 to 2.0, and 2.0 to 2.5 µm particle-size classes are shown. C/M (ordinate) expresses concentrations normalized to mass input (uranine) and particle number input (clay-loam suspension).

at very low levels, which may be due to the low injection quantities (the suspension mostly consisted of small particles, Figure S2). Therefore, the analysis will focus on smaller particles (0.9 to 3.5 µm) that were grouped into five size classes: 0.9 to 1.5, 1.5 to 2.0, 2.0 to 2.5, 2.5 to 3.0, and 3.0 to 3.5 µm. The first detection of these particles occurred 1.1 h after tracer release simultaneously to first uranine detection. Maximum concentrations of all size classes occurred simultaneously after 1.7 h, preceding the uranine peak by 26 min. The different size classes displayed short tails diminishing with increasing particle size. The total recovery of the injected particles decreased substantially with increasing particle size: 16.5%, 1.3%, 0.4%, 0.2%, and 0.1% recovery for the five different size classes mentioned earlier, respectively.

The earlier peak time of the 0.9 to 1.5 µm particles with respect to uranine is attributed to exclusion processes. Zhang et al. (2001) pointed out that an earlier peak time of particles with respect to solutes may also be an artifact due to a time-dependent particle-loss function by attachment and deposition. However, in the present case, the higher normalized concentrations of the finest particles with respect to uranine clearly demonstrate that particles are effectively transported at higher velocities than solutes. In porous media, particle mobility is constrained to the pore centers (size exclusion) and to accessible pore networks (pore exclusion) where flow velocities are highest, whereas solutes sample the entire pore volume. This results in an earlier breakthrough of particles (e.g., Ryan and Elimelech 1996; Sirivithayapakorn and Keller 2003). Similar processes also seem to occur in the unsaturated zone of a karst aquifer, that is, preferred particle transport in the centers of the larger pores and fractures.

The BTCs of the different size classes peaked simultaneously after 1.7 h. In contrast, similar tracing experiments carried out at the two other test sites (mentioned in the "Introduction" section), where soil is nearly absent, resulted in earlier breakthroughs of the larger particles with respect to fine particles. Apparently, the presence or absence of a soil cover has a significant influence on

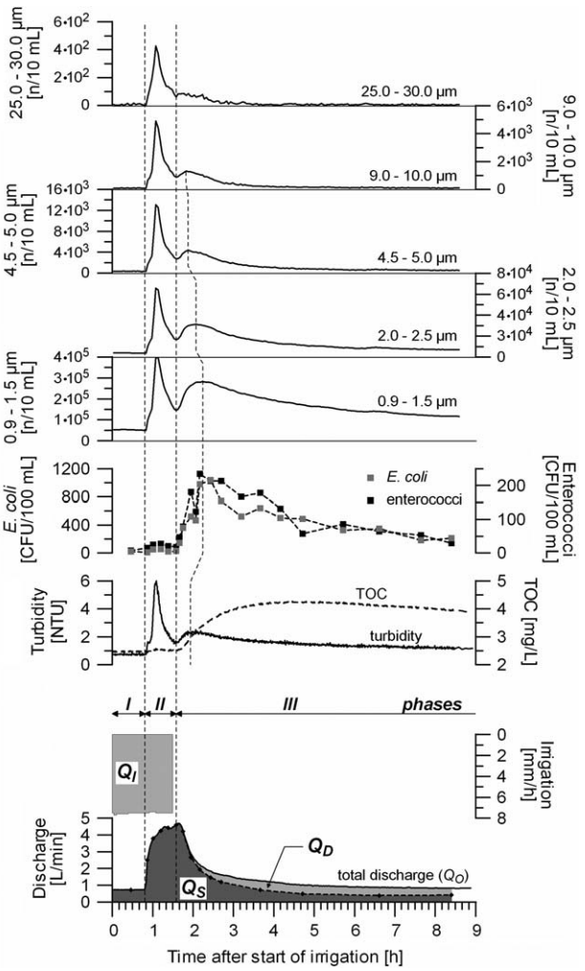

Figure 6. Temporal variations of natural parameters during the short-term irrigation experiment. Pulse-through turbidity is characterized by increases of all particle-size classes (phase II), whereas flow-through turbidity mainly shows increases of small particles (phase III).

preferential particle transport and exclusion mechanisms. Finally, the decreasing recovery for larger particles suggests increasing effectiveness of particle deposition mechanisms, such as mechanical filtration and straining (McDowellboyer et al. 1986).

Dynamics of Natural Particles and Fecal Bacteria during Transient Flow Regime

The outlet response to the short-term irrigation experiment (Figure 6), which was designed to simulate a natural rainfall event, has provided further insights into the transport of sediment particles, fecal bacteria, and TOC during transient flow conditions. The hydrograph and the temporal evolution of turbidity, TOC, and fecal bacteria (*E. coli* and enterococci) can also be divided into the three phases described previously: a lag period with stable preexperimental flow conditions and low levels of turbidity, TOC, and bacteria (lag phase, I); a discharge increase, strictly composed of epikarst storage water, coming along with a pulse-through turbidity peak but still

stable low levels of TOC and fecal bacteria (piston phase, II); and a mixed-flow period (epikarst storage water, soil water, and infiltration water) showing increases of turbidity (flow through), TOC, and bacteria (mixing phase, III). Because no steady-state flow regime was attained during this experiment, phase III could not be further subdivided.

PSD measurements allowed more detailed analyses of the turbidity signals. The pulse-through signal is characterized by a simultaneous evolution of all particle-size classes between 0.9 and 139 μm. In contrast, the flow-through signal is mainly composed of fine particles; this signal is blurred with larger size classes and no longer discernible at particle sizes more than 12 μm.

The peak times of the flow-through particles (phase III) preceded the TOC maximum, which is consistent with the findings of the artificial tracer test with particles and uranine described earlier. However, in this case, the peak times of the different particle-size classes increased systematically with decreasing particle size. The maximum concentration of the 9.0 to 10.0 μm particles occurred 25 min earlier than for the 0.9 to 1.5 μm particles, that is, large particles seem to travel at higher peak velocities (phase III). This finding suggests that the flow conditions in the unsaturated zone—steady state or transient state—also influence particle transport and exclusion mechanisms.

E. coli and enterococci are highly correlated to 0.9 to 1.5 μm particles during the flow-through turbidity period ($R^2 = 0.85$ and 0.87 for *E. coli* and enterococci, respectively). These results suggest similar origin, transport, and deposition processes for fecal bacteria and fine natural particles/colloids in the unsaturated zone. The same correlation was also observed at karst springs (Pronk et al. 2007). A relative increase of fine particles can thus be used as an early-warning parameter for fecal contamination.

Conclusions

The protection and management of water resources in karst aquifers require the understanding of water and contaminant transfer from the land surface through the entire hydrogeological system toward springs or other drinking water abstraction points. The present study investigated the storage and percolation of water and transport processes in the unsaturated zone, with a particular focus on particles and fecal bacteria, which represent the most important contaminants in many karst water supplies.

Results confirm that, during rainfall events and irrigation experiments, most of the water initially discharging at the base of the unsaturated zone originates from the epikarst and is remobilized by a pressure pulse; this finding is in agreement with previous studies (Lee and Krothe 2001; Perrin et al. 2003). The substantial quantity of water stored in the soil and epikarst (110 mm in this case) can either contribute to ground water recharge (downward movement during precipitation periods) or be used by plants (upward movement during dry spring and summer periods). With increasing rainfall or irrigation intensity and duration, an increasing amount of freshly infiltrated water contributes to deep percolation; this water can transport considerable amounts of sediments and associated contaminants from the land surface and soil zone toward the active conduit network.

Particles discharging at the base of the unsaturated zone have two distinct origins: the pulse-through turbidity, which is a result of the suspension and scouring of particles from the fractures close to the observation point, is highly dependent on the hydrodynamics in the epikarst and transmission zone; its PSD is characterized by significant increases of all particle-size classes, ranging from colloidal size up to 0.1 mm or more. Conversely, the flow-through turbidity, which corresponds to the arrival of soil particles mobilized especially during the first flush of storm rainfall events, is dependent on the flow-through time; its PSD is characterized by increases of the finer size classes, up to a few micrometers. This flow-through turbidity is often associated with high levels of fecal bacteria and TOC, which also originate from the land surface and underlying soil horizons.

A comparative tracer test with clayey loam suspension and uranine revealed that mineral particles tend to travel faster than solutes. Similarly, fecal bacteria often reach their maximum concentration before TOC. These findings indicate that exclusion processes, which are known from saturated porous media, also occur in the soil and unsaturated zone of a karst aquifer.

Fecal bacteria, which have sizes of about 1 μm, are very well correlated with fine particles (0.9 to 1.5 μm) during flow-through turbidity periods ($R^2 > 0.8$). A similar correlation was also observed in saturated conduit networks at karst springs affected by microbial contamination from swallow holes (Pronk et al. 2007). Results presented in this study thus confirm the use of continuous PSD monitoring as a reliable and sensitive early-warning parameter for potential microbial contamination of karst water, particularly if this contamination results from agricultural or other activities at the land surface and is flushed into the aquifer during storm rainfall events. The applicability of this approach to other type of microbial contamination, such as permanent waste water releases via leaking sewers or septic tanks, still needs to be tested.

Acknowledgments

We thank François Bourret, Ludovic Savoy, and Alain Pochon for technical and logistic support and David Drew for providing the final language check. The Swiss National Science Foundation (BEKARST/KARSTDYN, grant no 200020-113609/1) and the Canton of Solothurn funded this study.

Supporting Information

Additional Supporting Information may be found in the online version of this article.

Figure S1. Cumulative percentage frequency of particle-size distribution between 0.9 and 139 μm of the

clayey loam suspension released for the comparative tracer test during the long-term irrigation experiment.

Figure S2. Quantification of infiltration water discharging at the outlet (Q_D) during a long-term irrigation experiment calculated by means of chloride and bromide concentrations. Both methods give highly similar results. For both tracers, the calculated total volume of infiltration water discharged at the outlet (V_D) is 1.8 m^3 during this experiment. Cl^- in infiltration water: 9.6 mg/L; Cl^- in storage water: 1.3 mg/L; Br^- in infiltration water: 14.7 mg/L; and Br^- in storage water: 0.0 mg/L.

Figure S3. Relationship between the outlet discharge (Q) and the flow-through time (FT_t) obtained from artificial and natural tracer tests. Flow-through times are spans of time between the moment of discharge increase (for natural parameters) at the outlet or at the time of injection (for artificial tracers during long-term irrigation experiments) and the time when the respective parameter started to increase at the outlet.

References

American Public Health Association, American Water Works Association, and Water Environment Federation (APHA, AWWA, and WEF). 2005. *Standard Methods for the Examination of Water and Wastewater*, 21st ed. Alexandria, Virginia: Water Environment Federation.

Atteia, O., and R. Kozel. 1997. Particle size distributions in waters from a karstic aquifer: From particles to colloids. *Journal of Hydrology* 201, no. 1–4: 102–119.

Göppert, N., and N. Goldscheider. 2008. Solute and colloid transport in karst conduits under low- and high-flow conditions. *Ground Water* 46, no. 1: 61–68.

Herman, E.K., J.H. Tancredi, L. Toran, and W.B. White. 2007. Mineralogy of suspended sediment in three karst springs. *Hydrogeology Journal* 15, no. 2: 255–266.

Klimchouk, A. 2004. Towards defining, delimiting and classifying epikarst: Its origin, processes and variants of geomorphic evolution. *Speleogenesis and Evolution of Karst Aquifers* 2, no. 1: 1–13.

Kogovšek, J. 1997. Water tracing tests in vadose zone. In *Tracer Hydrology* 97, ed. A. Kranjc, 167–172. Rotterdam, The Netherlands: Balkema.

Lee, E.S., and N.C. Krothe. 2001. A four-component mixing model for water in a karst terrain in south-central Indiana, USA. Using solute concentration and stable isotopes as tracers. *Chemical Geology* 179, no. 1–4: 129–143.

Loop, C.M., and W.B. White. 2001. A conceptual model for DNAPL transport in karst ground water basins. *Ground Water* 39, no. 1: 119–127.

Mahler, B.J., J.C. Personne, G.F. Lods, and C. Drogue. 2000. Transport of free and particulate-associated bacteria in karst. *Journal of Hydrology* 238, no. 3–4: 179–193.

Mahler, B.J., and F.L. Lynch. 1999. Muddy waters: Temporal variation in sediment discharging from a karst spring. *Journal of Hydrology* 214, no. 1–4: 165–178.

Massei, N., H.Q. Wang, J.P. Dupont, J. Rodet, and B. Laignel. 2003. Assessment of direct transfer and resuspension of particles during turbid floods at a karstic spring. *Journal of Hydrology* 275, no. 1–2: 109–121.

McCarthy, J.F., and L.D. McKay. 2004. Colloid transport in the subsurface: Past, present and future challenges. *Vadose Zone Journal* 3, no. 2: 326–337.

McDowellboyer, L.M., J.R. Hunt, and N. Sitar. 1986. Particle-transport through porous media. *Water Resources Research* 22, no. 13: 1901–1921.

Perrin, J. 2003. A conceptual model of flow and transport in a karst aquifer based on spatial and temporal variations of natural tracers. Ph.D. diss., Centre of Hydrogeology, University of Neuchâtel, Neuchâtel, Switzerland.

Perrin, J., P.-Y. Jeannin, and F. Zwahlen. 2003. Epikarst storage in a karst aquifer: A conceptual model based on isotopic data, Milandre test site, Switzerland. *Journal of Hydrology* 279, no. 1–4: 106–124.

Pronk, M., N. Goldscheider, and J. Zopfi. 2007. Particle-size distribution as indicator for fecal bacteria contamination of drinking water from karst springs. *Environmental Science and Technology* 41, no. 24: 8400–8405.

Pronk, M., N. Goldscheider, and J. Zopfi. 2006. Dynamics and interaction of organic carbon, turbidity and bacteria in a karst aquifer system. *Hydrogeology Journal* 14, no. 4: 473–484.

Ryan, J.N., and M. Elimelech. 1996. Colloid mobilization and transport in groundwater. *Colloids and Surfaces A-Physicochemical and Engineering Aspects* 107, 1–56.

Ryan, M., and J. Meiman. 1996. An examination of short-term variations in water quality at a karst spring in Kentucky. *Ground Water* 34, no. 1: 23–30.

Savoy, L. 2007. Use of natural and artificial reactive tracers to investigate the transfer of solutes in karst systems. Ph.D. diss., Centre of Hydrogeology, University of Neuchâtel, Neuchâtel, Switzerland.

Schnegg, P.-A., and R. Costa. 2003 Tracer tests made easier with field fluorometers. Technical note. *Bulletin d'Hydrogéologie* 20, 89–91.

Sirivithayapakorn, S., and A.A. Keller. 2003. Transport of colloids in saturated porous media: A pore-scale observation of the size exclusion effect and colloid acceleration. *Water Resources Research* 39, no. 4: 1109.

Vesper, D.J., and W.B. White. 2004. Spring and conduit sediments as storage reservoirs for heavy metals in karst aquifers. *Environmental Geology* 45, no. 4: 481–493.

Vesper, D.J., and W.B. White. 2003. Metal transport to karst springs during storm flow: An example from Fort Campbell, Kentucky/Tennessee, USA. *Journal of Hydrology* 276, no. 1–4: 20–36.

White, W.B. 2002. Karst hydrology: Recent developments and open questions. *Engineering Geology* 65, no. 2–3: 85–105.

Williams, P.W. 2008. The role of the epikarst in karst and cave hydrogeology: A review. *International Journal of Speleology* 37, no. 1: 1–10.

Zhang, P., W.P. Johnson, M.J. Piana, C.C. Fuller, and D.L. Naftz. 2001. Potential artifacts in interpretation of differential breakthrough of colloids and dissolved tracers in the context of transport in a zero-valent iron permeable reactive barrier. *Ground Water* 39, no. 6: 831–840.

Zvikelsky, O., and N. Weisbrod. 2006. Impact of particle size on colloid transport in discrete fractures. *Water Resources Research* 42, no. 12: W12S08.